ACS Sustainable Chemistry & Engineering

Research Article

pubs.acs.org/journal/ascecg

Screening of Ionic Liquid/H_2O Working Pairs for Application in Low Temperature Driven Sorption Heat Pump Systems

Sabine Popp, Andreas Bösmann, René Wölfel, and Peter Wasserscheid*

Institute of Chemical Reaction Engineering, Friedrich-Alexander-University Erlangen-Nuremberg, Egerlandstraße 3, 91058 Erlangen, Germany

Supporting Information

ABSTRACT: Due to the known corrosion and crystallization issues of LiBr/H_2O, the state-of-the-art working pair in sorption heat pump (SHP) systems, research into alternative working pairs is of high practical relevance. We have studied a wide range of ionic liquids (ILs) for this application in order to find potential new systems with enhanced performance. The screening was conducted with a focus on vapor pressure measurements of, in total, 74 examined working pairs. As common vapor−liquid-equilibrium measurements are very precise but rather time-consuming, we developed a new setup allowing a fast relative determination of humidities with very small sample volumes for screening purposes. By this method we identified seventeen IL/H_2O working pairs fulfilling the technical relevant criterion of a water vapor pressure $p_{H_2O} \leq 10$ mbar at $T = 308$ K with an IL content of less than 80 wt % ($w_{IL} < 0.8$). Further evaluation of these candidates with respect to their thermal stability and viscosity allowed us to identify [MMIM][HCOO]/H_2O, [MMIM][OAc]/H_2O, [MMIM][C_2H_5COO]/H_2O, [Me_4N][HCOO]/H_2O, [Me_4N][OAc]/H_2O and [Me_4N] [C_2H_5COO]/H_2O as the most promising IL/H_2O systems for a possible application in SHP systems.

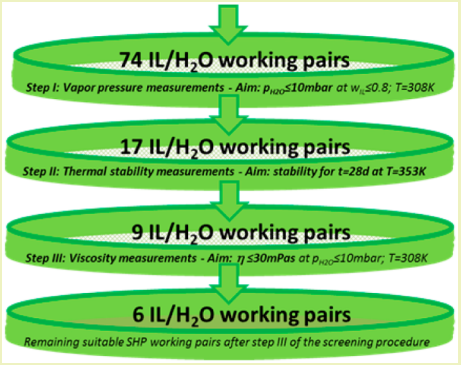

KEYWORDS: *Ionic liquid, Sorption heat pump, Vapor pressure, Thermal stability*

INTRODUCTION

One of the great challenges of science in our time is the development of energy production, storage and transformation systems with minimal ecological footprints. In this context, the growing demand for cooling energy calls for efficient technologies that can use low-caloric heat streams, for example from solar thermal installations, for cooling or heating. Consequently, thermally driven sorption heat pumps (SHPs), respectively absorption chillers, become more and more relevant. In SHPs, low temperature waste heat is leveled up to a higher temperature heat, which opens different and more valuable technical uses for this heat at the enhanced temperature level. Furthermore, the process cools part of the system down, and this low level temperature level can be used for energy-efficient cooling applications by absorption chillers. The SHP technology is already widely used in industry. As operating energy, waste heat from industrial processes, heat from combined heat and power (CHP) plants or hot water from solar or geothermal sources is applied.[1] However, the state-of-the-art working pairs, namely LiBr/H_2O and H_2O/NH_3, are characterized by some drawbacks. LiBr/H_2O has a high corrosion potential and tends to crystallize.[2,3] NH_3/H_2O is toxic and thus requires safeguards against accidental release. Furthermore, it has to be purified from water by rectification, a fact that results in high system costs.

To identify suitable alternative working pairs to LiBr/H_2O, a lot of research has been carried out over the past years. Besides research dealing with suitable salt-water mixtures,[4−7] a special focus was put on ionic IL/H_2O working pairs.[8−15] By choosing the proper cation−anion pair, the physical properties of the IL can be tuned toward the technically desired range.[16] Thus, using an IL as an absorption medium offers a realistic chance to overcome the crystallization and corrosion problems of the commercial working pair LiBr/H_2O. Several IL/H_2O systems were proposed as promising candidates for the application in SHP.[10] Among them, the working pair 1,3-dimethylimidazolium dimethylphosphate ([MMIM][DMP])/H_2O was intensively studied and vapor−liquid-equilibrium (VLE) data,[9,15,17,18] thermodynamic properties[9] as well as performance predictions in absorption refrigeration cycles were published.[15,17,19] The simulation results of Dong et al. even predict similar COP values for [MMIM][DMP]/H_2O compared to the common working pair LiBr/H_2O.[17]

The most important property for the identification of alternative IL-based working pairs for SHP systems is the reduction of water vapor pressure in the presence of the respective IL as probed by vapor−liquid - equilibrium (VLE) measurements. Dong et al. carried out vapor pressure measurements for [MMIM][DMP]/H_2O by the boiling point method.[17] Römrich et al. performed the VLE measurements for 1-ethyl-3-methylimidazolium acetate ([EMIM][OAc])/H_2O and diethylammonium methanesulfonate ([DEMA][OMs])/

Received: January 25, 2015
Revised: March 14, 2015
Published: March 25, 2015

DOI: 10.1021/acssuschemeng.5b00062
ACS Sustainable Chem. Eng. 2015, 3, 750−757

Table 1. Overview of the Screened Ionic Liquids

N°	name	abbreviation
1	(2-hydroxyethyl)dimethylammonium acetate	[$Me_2EtOHNH$][OAc]
2	(2-hydroxyethyl)dimethylammonium nitrate	[$Me_2EtOHNH$][NO_3]
3	(2-hydroxyethyl)methylammonium acetate	[$MeEtOHNH_2$][OAc]
4	(2-hydroxyethyl)methylammonium nitrate	[$MeEtOHNH_2$][NO_3]
5	(2-hydroxyethyl)trimethylammonium acetate	[Me_3EtOHN][OAc]
6	(2-hydroxyethyl)trimethylammonium butyrate	[Me_3EtOHN][butyrate]
7	(2-hydroxyethyl)trimethylammonium chloracetate	[Me_3EtOHN][ClOAc]
8	(2-hydroxyethyl)trimethylammonium formate	[Me_3EtOHN][HCOO]
9	(2-hydroxyethyl)trimethylammonium fumarate	[Me_3EtOHN][fumarate]
10	(2-hydroxyethyl)trimethylammonium glycinate	[Me_3EtOHN][glycinate]
11	(2-hydroxyethyl)trimethylammonium glycolate	[Me_3EtOHN][glycolate]
12	(2-hydroxyethyl)trimethylammonium hydrogennitrate	[Me_3EtOHN][HNO_3]
13	(2-hydroxyethyl)trimethylammonium hydrogensulfate	[Me_3EtOHN][HSO_4]
14	(2-hydroxyethyl)trimethylammonium sulfite	[Me_3EtOHN][SO_3]
15	(2-hydroxyethyl)trimethylammonium hydrogensulfite	[Me_3EtOHN][HSO_3]
16	(2-hydroxyethyl)trimethylammonium isobutyrate	[Me_3EtOHN][isobutyrate]
17	(2-hydroxyethyl)trimethylammonium lactate	[Me_3EtOHN][lactate]
18	(2-hydroxyethyl)trimethylammonium maleate	[Me_3EtOHN][maleate]
19	(2-hydroxyethyl)trimethylammonium malonate	[Me_3EtOHN][malonate]
20	(2-hydroxyethyl)trimethylammonium methylsulfonate	[Me_3EtOHN][$MeSO_3$]
21	(2-hydroxyethyl)trimethylammonium oxalate	[Me_3EtOHN][oxalate]
22	(2-hydroxyethyl)trimethylammonium perchlorate	[Me_3EtOHN][PerCl]
23	(2-hydroxyethyl)trimethylammonium propionate	[Me_3EtOHN][C_2H_5COO]
24	(2-hydroxyethyl)trimethylammonium pyruvate	[Me_3EtOHN][pyruvate]
25	(2-hydroxyethyl)trimethylammonium succinate	[Me_3EtOHN][succinate]
26	(2-hydroxyethyl)trimethylammonium sulfate	[Me_3EtOHN][SO_4]
27	(2-hydroxyethyl)trimethylammonium trifluoroacetate	[Me_3EtOHN][TFA]
28	(2-hydroxyethyl)trimethylammonium trifluoromethylsulfonate	[Me_3EtOHN][CF_3SO_3]
29	(2-hydroxyethyl)trimethylammonium nitrate	[Me_3EtOHN][NO_3]
30	1,3-dimethylimidazolium acetate	[MMIM][OAc]
31	1,3-dimethylimidazolium butyrate	[MMIM][butyrate]
32	1,3-dimethylimidazolium chloracetate	[MMIM][ClOAc]
33	1,3-dimethylimidazolium formate	[MMIM][HCOO]
34	1,3-dimethylimidazolium glycolate	[MMIM][glycolate]
35	1,3-dimethylimidazolium hydrogensulfate	[MMIM][HSO_4]
36	1,3-dimethylimidazolium hydrogensulfite	[MMIM][HSO_3]
37	1,3-dimethylimidazolium isobutyrate	[MMIM][isobutyrate]
38	1,3-dimethylimidazolium lactate	[MMIM][lactate]
39	1,3-dimethylimidazolium methanesulfonate	[MMIM][$MeSO_3$]
40	1,3-dimethylimidazolium nitrate	[MMIM][NO_3]
41	1,3-dimethylimidazolium propionate	[MMIM][C_2H_5COO]
42	1,3-dimethylimidazolium sulfite	[MMIM][SO_3]
43	ammonium acetate	[NH_4][OAc]
44	ammonium nitrate	[NH_4][NO_3]
45	dimethylammonium acetate	[Me_2NH_2][OAc]
46	dimethylammonium nitrate	[Me_2NH_2][NO_3]
47	methylammonium acetate	[$MeNH_3$][OAc]
48	methylammonium nitrate	[$MeNH_3$][NO_3]
49	tetrabutylphosphonium acetate	[Bu_4P][OAc]
50	tetrabutylphosphonium nitrate	[Bu_4P][NO_3]
51	tetramethylammonium acetate	[Me_4N][OAc]
52	tetramethylammonium butyrate	[Me_4N][butyrate]
53	tetramethylammonium formate	[Me_4N][HCOO]
54	tetramethylammonium glycolate	[Me_4N][glycolate]
55	tetramethylammonium hydrogensulfite	[Me_4N][HSO_3]
56	tetramethylammonium isobutyrate	[Me_4N][isobutyrate]
57	tetramethylammonium lactate	[Me_4N][lactate]
58	tetramethylammonium nitrate	[Me_4N][NO_3]
59	tetramethylammonium propionate	[Me_4N][C_2H_5COO]
60	tetramethylammonium sulfite	[Me_4N][SO_3]
61	trimethylammonium acetate	[Me_3NH][OAc]
62	trimethylammonium nitrate	[Me_3NH][NO_3]
63	trimethylsulfonium acetate	[Me_3S][OAc]
64	trimethylsulfonium butyrate	[Me_3S][butyrate]
65	trimethylsulfonium formate	[Me_3S][HCOO]
66	trimethylsulfonium glycolate	[Me_3S][glycolate]
67	trimethylsulfonium hydrogensulfite	[Me_3S][HSO_3]
68	trimethylsulfonium isobutyrate	[Me_3S][isobutyrate]
69	trimethylsulfonium lactate	[Me_3S][lactate]
70	trimethylsulfonium propionate	[Me_3S][C_2H_5COO]
71	trimethylsulfonium sulfate	[Me_3S][SO_4]
72	trimethylsulfonium sulfite	[Me_3S][SO_3]
73	(2-hydroxyethyl)ammonium acetate	[$EtOHNH_3$][OAc]
74	(2-hydroxyethyl)ammonium nitrate	[$EtOHNH_3$][NO_3]

H_2O in a dynamic measurement apparatus.[12] Kato and Gmehling designed a computer-driven static ebulliometer method for very accurate VLE measurements of, e.g., 1-ethyl-3-methylimidazolium bis(trifluoromethylsulfonyl)imide ([EMIM][NTf_2])/H_2O or [MMIM][DMP]/H_2O.[18] The group of Calvar examined VLE of ternary systems like 1-butyl-3-methylimidazolium methylsulfate ([BMIM][$MeSO_4$])/H_2O/EtOH with a dynamic recirculating distillation apparatus.[20]

Those techniques provide relatively exact vapor pressure values with mean uncertainties of about ±0.52%[17]−±2.4%.[12] However, these methods need relatively large sample volumes (V = 70[12]−250 mL[17]), leading to both expenses in material and long times until equilibrium in the measurement cell is reached. Thus, those methods are not really suitable for a fast screening of a wide range of IL/H_2O working pairs.

In this contribution, we present a new experimental setup for the fast screening of a large number of potentially interesting working pairs for SHP systems. The applied apparatus measures simultaneously relative humidity and temperature. The here described method is simple compared to common VLE measurements and can be performed with very small sample volumes (V = 1 mL) and very little pre-experimental effort. The new setup also allows the parallel measurement of

DOI: 10.1021/acssuschemeng.5b00062
ACS Sustainable Chem. Eng. 2015, 3, 750−757

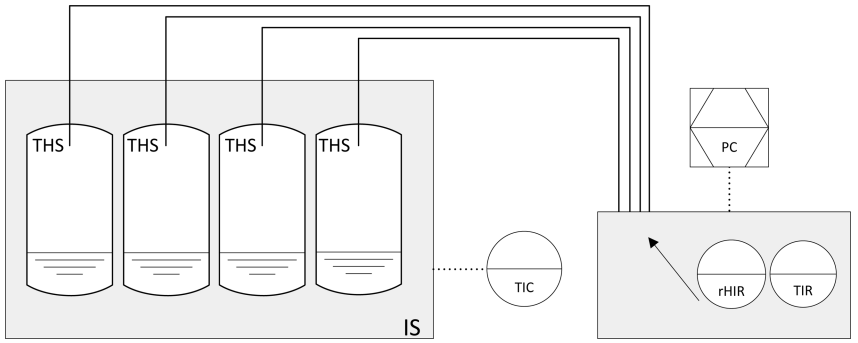

Figure 1. Relative humidity measurement apparatus: THS, temperature and humidity sensor; IS, incubator and shaker unit; TIC, temperature indicator and control in incubator and shaker unit; rHIR TIR, indication and recording of relative humidity and temperature.

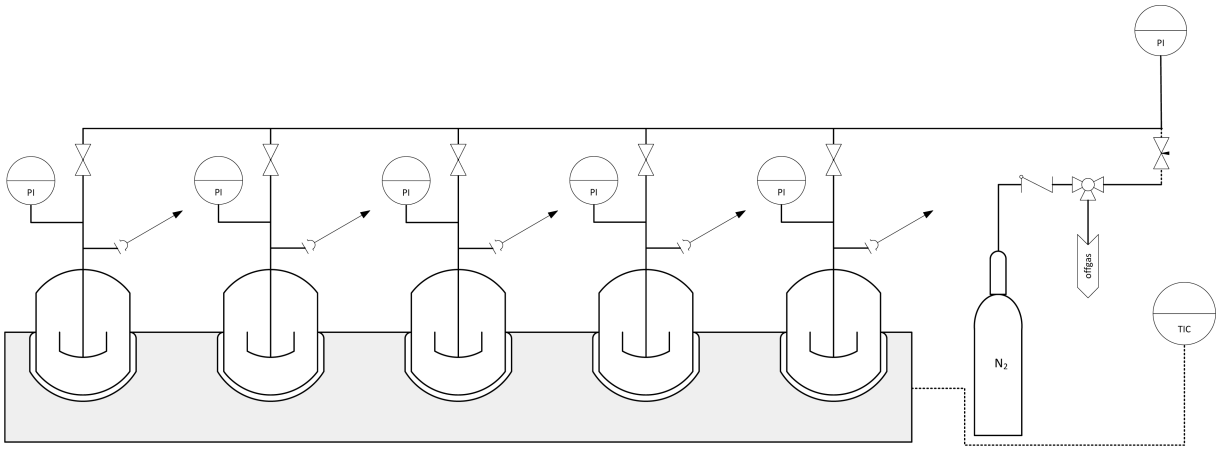

Figure 2. Autoclave apparatus for thermal stability measurements.

16 IL/water samples making the screening process even more effective. The screening experiments described in this contribution include 74 different ILs, each of which was measured in various concentrations in water. Besides the results of relative humidity measurements, we further present thermal stability and viscosity data for the six most promising IL/H_2O working pairs.

EXPERIMENTAL SECTION

Materials and Purities. All ILs under investigation (see Table 1) were synthesized by acid/base reactions. The base (in aqueous or methanolic solution) was placed in a round-bottom flask and cooled in ice water. Then, equimolar amounts of the respective acid were added dropwise while stirring. After addition, the ice bath was removed and stirring was further conducted for t = 1 h. After the end of the reaction, the methanol/water solvent was removed from the IL using a rotary evaporator at p = 10 mbar and T = 60 °C. The purity of the synthesized ILs was checked by ^{1}H NMR measurements and was determined to >98% for all synthesized ILs. Water contents were determined by Karl Fischer titration (KF Coulometer 756, Metrohm). The water contents were measured, in order to prepare the samples precisely in the desired compositions and for precise viscosity measurements.

For further information about the used chemicals and the list of supplier of the commercially available materials, see the Supporting Information.

Apparatus and Procedure. *Measurements of Relative Humidity.* The relative humidity measurements were carried out in a static apparatus, exemplarily shown with 4 instead of 16 measurement ports, in Figure 1. The apparatus consists of an incubating mini shaker (VWR, T = RT−65 °C, shaking speed = 100−900 rpm) and a tube rack, where up to 16 sample vials can be clamped in. The sample vials are headspace screw neck vials with precision thread (V_{vial} = 10 mL). The simultaneous temperature (T) and relative humidity (rH) measurements of the gas phase above the sample is carried out by a capacitive polymer sensor (SENSIRION, SHT75) with an accuracy of T = ± 0.4 K and ±1.8% rH.[21] Each sensor is fused in a matching screw cap for the vial, so that the vial is hermetically sealed during the relative humidity measurement. Data logging of T and rH values is performed by using the evaluation software EK-H4 Viewer (SENSIRION, EK-H4) and a computer. The commercially available evaluation kit, which includes an evaluation unit for 4 sensor channels, was extended by a 4-fold switch to allow the measurement of up to 4 × 4 samples simultaneously.

The water vapor pressure over the IL solutions (p_{H_2O}) was calculated from the measured relative humidity (% rH), the temperature (T) and the saturated vapor pressure of water (e_w)[22] using the Magnus equation.

see ref 22

$$e_w(T) = 6.1078 \cdot \exp\left(\frac{17.08085 \cdot T}{234.175 + T}\right) \quad (1)$$

see ref 22

$$\%\mathrm{rH} = \frac{p_{H_2O}(T)}{e_w(T)} \cdot 100 \quad (2)$$

$$p_{H_2O}(T) = \frac{\%\mathrm{rH}}{100} \cdot 6.1078 \cdot \exp\left(\frac{17.08085 \cdot T}{234.175 + T}\right) \quad (3)$$

For the relative humidity measurements, each IL/H_2O working pair was prepared in 4 different compositions between 60 and 90 wt % IL. Each vial was filled with V = 1 mL of the respective sample and closed with the appropriate sensor cap. The temperature and shaker speed

DOI: 10.1021/acssuschemeng.5b00062
ACS Sustainable Chem. Eng. 2015, 3, 750−757

Table 2. Matrix of Screened ILs in Combination with H_2O against the Technical Criterion of $p_{H2O} \leq 10$ mbar (± 2 mbar) at $T = 308$ K and $w_{IL} < 0.8$[a]

	[$Me_2EtOHNH$]	[$MeEtOHNH_2$]	[Me_3EtOHN]	[MMIM]	[NH_4]	[Me_2NH_2]	[$MeNH_3$]	[Bu_4P]	[Me_4N]	[Me_3NH]	[Me_3S]	[$EtOHNH_3$]
[butyrate]			−	+					+		+	
[CF_3SO_3]			−	−								
[ClOAc]			−	−								
[HCOO]			+	+					+		+	
[fumarate]			−									
[glycinate]			−									
[glycolate]			−	−					+		−	
[HNO_3]			−									
[HSO_3]			−	−					−		+	
[HSO_4]			−	−								
[isobutyrate]			−	+					+		+	
[lactate]			−	−					+		−	
[malonate]			−									
[$MeSO_3$]			−	+								
[maleate]			−									
[NO_3]	−	−	−	−	−	−	−	−	−	−		−
[OAc]	−	−	+	+	−	−	−	−	+	−	+	−
[oxalate]			−									
[PerCl]			−									
[C_2H_5COO]			+	+					+		+	
[pyruvate]			−									
[SO_3]			−	−					+		−	
[SO_4]			−								−	
[succinate]			−									
[TFA]			−									

[a](+) = does fulfill the criterion, (−) = does not fulfill the criterion.

DOI: 10.1021/acssuschemeng.5b00062
ACS Sustainable Chem. Eng. 2015, 3, 750−757

were set, and the data logging was started. After about t = 45 min, the equilibrium humidity was reached in the gas phase and the measurement was stopped. Before and after the experiments, the sensors were always checked for accuracy. Deviating sensors were replaced, and the measurement of the respective sample was discarded. Furthermore, the reliability of the measurements was checked by comparing literature vapor pressure data from LiBr/H_2O and pure water[23,24] with measured vapor pressure data at T = 303 K. The mean uncertainty between literature and measured vapor pressure data of LiBr/H_2O in the range between 40 and 55 wt % LiBr was determined to ±11.1%. The mean uncertainty between measured and literature vapor pressure data for water at T = 303 K was determined to ±2.4%.

Thermal Stability Measurements. Thermal stability measurements of the working pairs were carried out in a mini autoclave setup, shown in Figure 2. It consists of 10 autoclaves, which are made of stainless steel (1.4571). Each autoclave had a volume of V = 21 mL. The autoclaves were put in a heatable aluminum block, the temperature control of which was ensured by a PID controller HT MC1 (Horst). Mixing of the samples in the autoclaves was realized by a 10-fold magnetic stirrer, which was arranged underneath the heating block. Each autoclave was sealed with a Viton O-ring. A burst-disk was assembled on each reactor. For inertization of the gas phase, the pressure vessels were connected with a gas distribution system. With the appropriate valve position, inert gas could be filled into the autoclaves or the pressure in the vessels could be purged.

Thermal stability measurements of the IL/H_2O working pairs were carried out at T = 353 K for t = 28 d. The temperature was chosen according to the temperature level in steam driven absorption heat pump systems.[25] Each sample was prepared by weighing m = 5 g in a glass liner; blank tests were taken for headspace-gas chromatography (GC) and NMR measurements. Afterward, the samples were placed into an autoclave. The pressure vessel was closed, connected with the inert gas distribution system and the autoclave was flushed three times with nitrogen. After the gas phase was inertized above the sample, the temperature was set to T = 353 K. After t = 7, 14, 21 and 28 d, the autoclave was cooled down and samples were taken and analyzed by ^{1}H NMR and headspace-GC. Afterward, the autoclave was closed, inertized and heated up again.

Viscosity Measurements. The viscosity measurements were carried out in a cone−plate Rheometer (Paar Physica MCR100). Samples were measured at T = 303−353 K and at shear rates of $\dot{\gamma}$ = 1−2000 s^{-1}.

RESULTS AND DISCUSSION

To find alternative IL/H_2O working pairs with enhanced efficiency for the application in sorption heat pump (SHP) systems, a systematic screening approach was chosen. To this end, a range of 74 ILs was synthesized by acid−base reactions. Some of the synthesized salts represent "poor" ILs, as described by Yoshizawa.[26] It is expected that those salts do not perform well in our screening. The initial preselection was based on the relative humidity measurements in our new screening apparatus to verify the reduction of vapor pressure of the refrigerant (H_2O) in the absorbent (IL). After data evaluation, we selected the working pairs with the lowest vapor pressure values. The second essential requirement for suitable working pairs is robustness, i.e., thermal stability at SHP working conditions. After identification of the thermally stable working pairs, further physical properties were determined for those working pairs that passed the previous tests.

Our screening included a variety of ILs with highly hydrophilic ions and excluded highly corrosive anions. Sets of cations were initially screened with $[NO_3]^-$ and $[OAc]^-$ ions. After the results were evaluated, the best performing cations were selected and screened with organic and inorganic hydrophilic anions. All IL/H_2O working pairs studied (see Table 1) were benchmarked against the technical goal of providing a water vapor pressure $p_{H_2O} \leq 10$ mbar at T = 308 K with less than 80 wt % ($w_{IL} < 0.8$) IL. Temperature and pressure values of this technical goal were chosen to correspond to the average absorber conditions in a LiBr/H_2O driven sorption heat pump system.[25,27,28] This match is important to facilitate a drop-in replacement of LiBr by the identified best IL in existing SHP systems. The maximum IL fraction criterion in the technical goal is derived from the fact that at very high IL fraction the viscosity of the IL absorbent would be too high to enable efficient heat transfer processes. The matrix shown in Table 2 illustrates the cation−anion pairs which were found to fulfill the technical goal of $p_{H_2O} \leq 10$ mbar (±2 mbar) at T = 308 K and $w_{IL} < 0.8$. The working pairs signed with (−) were either not soluble under the desired conditions or did not lower the vapor pressure to p_{H_2O} = 10 mbar at any composition. The blank fields in Table 2 indicate that those cation−anion pairs were not tested. Detailed vapor pressure data for all measured systems can be found in the Supporting Information.

As the result of this screening, 24 IL/H_2O working pairs (see Table 2 (+)) were identified to fulfill the set criterion. From these, 17 working pairs reaching $p_{H_2O} \leq 10$ mbar at the lowest IL fraction were selected for further characterization of their thermal stability and viscosity at the relevant water contents. An IL is regarded as thermally unstable if decomposition products can be found by NMR or headspace-GC−MS. No attempt was made to derive decomposition kinetics. Table 3 shows the results of the long-term stability tests under vapor atmosphere and close to realistic SHP working conditions at T = 353 K for 28 days.

Table 3. Results of the Thermal Stability Test of 17 Ionic Liquid/H_2O Working Pairs[a]

	[MMIM]	[Me_3S]	[Me_4N]
[HCOO]	+	−	+
[OAc]	+	−	+
[C_2H_5COO]	+	−	+
[butyrate]	−	−	+
[isobutyrate]	−	−	+
[glycolate]			+
[lactate]			−

[a]Measurements were carried out at T = 353 K for 28 days: (+) = stable, (−) = unstable according to ^{1}H NMR and headspace-GC−MS analytics.

All examined sulfonium ILs, as well as [MMIM][butyrate], [MMIM][isobutyrate] and [Me_4N][lactate], turned out to be unstable under these test conditions. After only 7 days of testing, all of these systems showed clear signs of decomposition both in the liquid (^{1}H NMR spectra) and the gas phase (headspace-GC chromatograms). Amines and alkyl esters were identified as main decomposition products, indicating that cation dealkylation is the main decomposition mechanism. A detailed study on decomposition mechanism and kinetics of imidazolium salts was published by Keil et al.[29]

In a next set of experiments, the viscosities of the nine systems that had passed the water vapor test and the stability test were determined. For these tests, typical compositions of the tested IL/H_2O working pairs at absorber temperature T = 308 K and at generator temperature T = 353 K were examined. The corresponding data are shown in Table 4.

DOI: 10.1021/acssuschemeng.5b00062
ACS Sustainable Chem. Eng. 2015, 3, 750−757

Table 4. Experimental Dynamic Viscosity Data for Selected Working Pairs IL (1)−water (2) at T = 308 K and T = 353 K

		η (mPa·s)	
ionic liquid (1)	w_1	T = 308 K	T = 353 K
[MMIM][HCOO]	0.770	8.01	3.5
[MMIM][OAc]	0.785	14.9	4.8
[MMIM][C_2H_5COO]	0.786	18.7	5.8
[Me_4N][HCOO]	0.712	10.4	4.2
[Me_4N][OAc]	0.717	28.4	7.1
[Me_4N][C_2H_5COO]	0.732	29.2	7.5
[Me_4N][butyrate]	0.752	43.2	9.4
[Me_4N][isobutyrate]	0.795	62.5	11.5
[Me_4N][glycolate]	0.801	35.8	8.3

All working pairs listed in Table 4 showed Newtonian behavior. The viscosity profile over the temperature range T = 303−353 K for the working pairs shown in Table 4 is plotted in Figure 3.

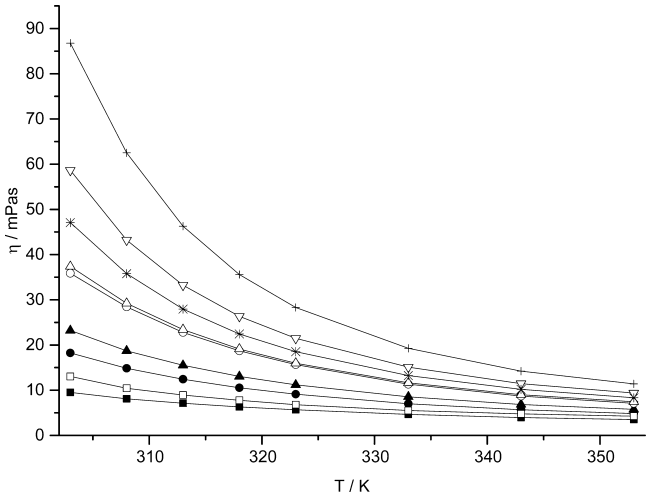

Figure 3. Dynamic viscosity versus temperature T = 303−353 K for ■ [MMIM][HCOO] + H_2O, ● [MMIM][OAc] + H_2O, ▲ [MMIM]-[C_2H_5COO] + H_2O, □ [Me_4N][HCOO] + H_2O, ○ [Me_4N][OAc] + H_2O, △ [Me_4N][C_2H_5COO] + H_2O, ▽ [Me_4N][glycolate] H_2O, + [Me_4N][butyrate] + H_2O, ∗ [Me_4N][isobutyrate] + H_2O; for compositions, see Table 4.

The values for dynamic viscosities decrease, as expected, with increasing temperature. As low viscosities are highly relevant for the heat transfer properties of the absorbent and thus for the dimensions for the cooling apparatus, we restricted the final, detailed investigation of the relative humidities to those six IL absorbents that reach a viscosity of less than 30 mPa·s at T = 308 K at the water content corresponding to $p_{H_2O} \leq 10$ mbar.

Under these selection criteria, six ionic liquids have been identified as promising candidates for future SHP applications. Table 5 gives for these six ILs the detailed results of the relative humidity measurements. Figure 4 displays the corresponding vapor pressure curves for the working pairs at different IL fractions between w_{IL} = 0.55−0.90.

Comparing ionic liquids of different cation types, it becomes obvious from the obtained data that ILs with the $[Me_4N]^+$ ion show lower vapor pressure values over the whole composition range compared to working pairs with the $[MMIM]^+$ ion. Furthermore, it is noteworthy that none of the IL/H_2O systems studied showed any sign of crystallization in the measured composition range (see Table 5). The anions $[HCOO]^-$, $[OAc]^-$ and $[C_2H_5COO]^-$ show similar vapor pressure values in combination with both cations.

Table 5. Experimental Relative Humidities and Temperature Data for Six Systems Ionic Liquid (1)−Water (2) and Calculated Water Vapor Pressures

ionic liquid (1)	w_1	rH (%)	T (K)	p_{H_2O} (mbar)
[MMIM][HCOO]	0.804	12.41	307.97	6.92
	0.794	15.21	307.22	8.13
	0.742	24.54	307.18	13.09
	0.719	28.06	307.95	15.62
	0.687	36.68	308.15	20.65
	0.595	55.33	308.99	32.63
[MMIM][OAc]	0.885	4.26	308.43	2.43
	0.830	11.97	307.48	6.50
	0.787	19.14	307.47	10.38
	0.740	28.19	307.82	15.59
	0.699	36.29	308.19	20.47
	0.645	45.80	308.97	26.98
[MMIM][C_2H_5COO]	0.803	12.79	307.20	6.83
	0.785	15.56	307.38	8.40
	0.714	27.12	308.11	15.23
	0.689	33.13	307.81	18.30
	0.629	43.98	307.21	23.51
	0.599	50.17	307.61	27.41
[Me_4N][HCOO]	0.749	14.15	307.37	7.63
	0.710	17.55	307.84	9.71
	0.676	22.85	308.39	13.03
	0.636	31.31	308.49	17.96
	0.593	41.93	307.27	22.49
	0.566	47.71	307.47	25.87
[Me_4N][OAc]	0.776	11.58	307.74	6.38
	0.734	15.19	308.26	8.61
	0.726	16.60	308.33	9.44
	0.696	21.32	308.34	12.13
	0.659	26.16	308.27	14.83
	0.624	33.39	308.88	19.56
[Me_4N][C_2H_5COO]	0.776	12.11	308.58	6.98
	0.768	13.08	308.36	7.45
	0.732	18.12	308.67	10.49
	0.694	23.58	308.51	13.54
	0.661	28.23	308.24	15.98
	0.590	41.50	308.16	23.38

CONCLUSION

In this work, we have presented a fast and efficient screening method to identify promising IL/H_2O working pairs for application in SHP systems. The first preselection from a group of in total 74 ionic liquids was carried out based on water vapor pressure data obtained from a simple screening apparatus measuring simultaneously vapor pressure and temperature in a highly parallelized manner using small sample volumes of 1 mL per sample. The criterion for the preselection was set at a maximum water vapor pressure of 10 mbar at T = 308 K with not more than 80 wt % IL present in the respective mixture. This criterion is closely related to the requirements of a drop-in replacement of LiBr by the newly developed IL in existing equipment. Seventeen IL/H_2O systems were found to pass the criterion and were further investigated in thermal stability tests and viscosity tests. Only six candidates turned out to remain

DOI: 10.1021/acssuschemeng.5b00062
ACS Sustainable Chem. Eng. 2015, 3, 750−757

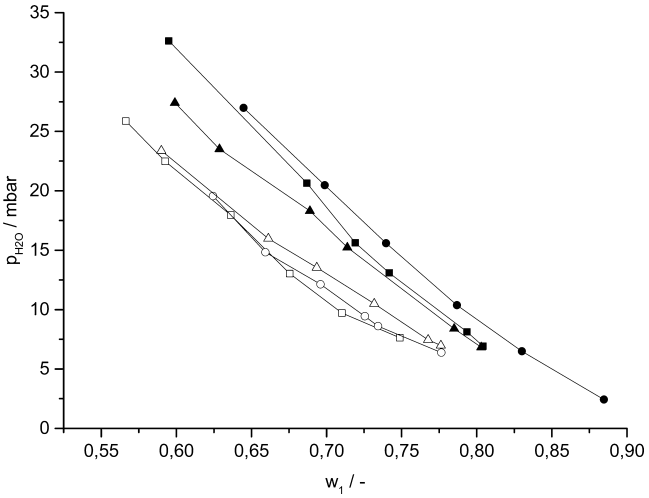

Figure 4. Comparison of vapor pressure data versus mass fraction of IL (1) at about T = 308 K: ■ [MMIM][HCOO] + H_2O, ● [MMIM][OAc] + H_2O, ▲ [MMIM][C_2H_5COO] + H_2O, □ [Me_4N][HCOO] + H_2O, ○ [Me_4N][OAc] + H_2O, △ [Me_4N]-[C_2H_5COO] + H_2O.

stable in the presence of water vapor at 353 K for 28 days and showed a dynamic viscosity of less than 30 mPa·s at SHP absorber conditions. These six IL candidates are proposed as suitable candidates in future IL/H_2O working pairs for SHP systems and merit in our views a more detailed investigation and potentially a technical development for this specific application: [MMIM][HCOO], [MMIM][OAc], [MMIM]-[C_2H_5COO], [Me_4N][HCOO], [Me_4N][OAc] and [Me_4N]-[C_2H_5COO].

■ ASSOCIATED CONTENT

Ⓢ Supporting Information

Additional information as noted in text. This material is available free of charge via the Internet at http://pubs.acs.org.

■ AUTHOR INFORMATION

Corresponding Author

*Peter Wasserscheid. E-mail: peter.wasserscheid@fau.de.

Notes

The authors declare no competing financial interest.

■ ACKNOWLEDGMENTS

The authors thank Marc-Christoph Schneider, Rolf Schneider, Sebastian Willmes and Olivier Zehnacker from Evonik Industries and Matthias Seiler for fruitful discussions. Furthermore, the German Federal Ministry of Education and Research is acknowledged for financial support within its public funded project, "Utilization of low caloric waste heat with sorption heat pump systems by ionic liquids and thermochemical storage (SIT 01RC1002B)". Support by the Energie Campus Nürnberg (www.encn.de) is in addition gratefully acknowledged.

■ REFERENCES

(1) YORK by Johnson Controls. Application opportunities for absorption chillers. http://www.johnsoncontrols.com/content/dam/WWW/jci/be/integrated_hvac_systems/hvac_equipment/chiller_products/absorption_single/Absorption_Single_Stage_Application_Guide_PDF.pdf (accessed 15/10/2014).

(2) Herold, K. E.; Radermacher, R.; Klein, S. A. *Absorption Chillers and Heat Pumps*; CRC Press: Boca Raton, FL, 1996.

(3) Brandt, B. Korrosionsverhalten ausgewählter werkstoffe in lithiumbromid-lösung für den anwendungsfall absorptionskältemaschinen. *Mater. Corros.* **2004**, *55*, 536−542.

(4) Macriss, R. A.; Zawacki, T. S. *Absorption Fluids Data Survey: Final Report on USA Data*; Institute of Gas Technology, U.S. Department of Energy: Chicago, IL, 1986.

(5) Lee, H. R.; Koo, K. K.; Jeong, S.; Kim, J. S.; Lee, H.; Oh, Y. S.; Park, D. R.; Baek, Y. S. Thermodynamic design data and performance evaluation of the water + lithium bromide + lithium iodide + lithium nitrate + lithium chloride system for absorption chiller. *Applied Therm. Eng.* **2000**, *20*, 707−720.

(6) De Lucas, A.; Donate, M.; Rodríguez, J. F. Absorption of water vapor into new working fluids for absorption refrigeration systems. *Ind. Eng. Chem. Res.* **2006**, *46*, 345−350.

(7) Koo, K.-K.; Lee, H.-R.; Jeong, S. Solubilities, vapor pressures, and heat capacities of the water + LiBr + $LiNO_3$ + LiI + LiCl System. *Int. J. Thermophys.* **1999**, *20*, 589−600.

(8) Wasserscheid, P.; Seiler, M. Leveraging gigawatt potentials by smart heat-pump technologies using ionic liquids. *ChemSusChem* **2011**, *4*, 459−463.

(9) He, Z.; Zhao, Z.; Zhang, X.; Feng, H. Thermodynamic properties of new heat pump working pairs: 1,3-Dimethylimidazolium dimethylphosphate and water, ethanol and methanol. *Fluid Phase Equilib.* **2010**, *298*, 83−91.

(10) Zheng, D.; Dong, L.; Huang, W.; Wu, X.; Nie, N. A review of imidazolium ionic liquids research and development towards working pair of absorption cycle. *Renewable Sustainable Energy Rev.* **2014**, *37*, 47−68.

(11) Seiler, M.; Kühn, A.; Ziegler, F.; Wang, X. Sustainable cooling strategies using new chemical system solutions. *Ind. Eng. Chem. Res.* **2013**, *52*, 16519−16546.

(12) Römich, C.; Merkel, N. C.; Valbonesi, A.; Schaber, K.; Sauer, S.; Schubert, T. J. S. Thermodynamic properties of binary mixtures of water and room-temperature ionic liquids: Vapor pressures, heat capacities, densities, and viscosities of water + 1-ethyl-3-methylimidazolium acetate and water + diethylmethylammonium methane sulfonate. *J. Chem. Eng. Data* **2012**, *57*, 2258−2264.

(13) Khamooshi, M.; Parham, K.; Atikol, U. Overview of ionic liquids used as working fluids in absorption cycles. *Adv. Mech. Eng.* **2013**, *2013*, 7.

(14) Constantinescu, D.; Schaber, K.; Agel, F.; Klingele, M. H.; Schubert, T. J. S. Viscosities, vapor pressures, and excess enthalpies of choline lactate + water, choline glycolate + water, and choline methanesulfonate + water systems. *J. Chem. Eng. Data* **2007**, *52*, 1280−1285.

(15) Yokozeki, A.; Shiflett, M. B. Water solubility in ionic liquids and application to absorption cycles. *Ind. Eng. Chem. Res.* **2010**, *49*, 9496−9503.

(16) Wasserscheid, P.; Welton, T. *Ionic Liquids in Synthesis*; Wiley-VCH: Weinheim, Germany, 2008.

(17) Dong, L.; Zheng, D.; Nie, N.; Li, Y. Performance prediction of absorption refrigeration cycle based on the measurements of vapor pressure and heat capacity of H_2O&[DMIM]DMP system. *Appl. Energy* **2012**, *98*, 326−332.

(18) Kato, R.; Gmehling, J. Measurement and correlation of vapor−liquid equilibria of binary systems containing the ionic liquids [EMIM][$(CF_3SO_2)_2N$], [BMIM][$(CF_3SO_2)_2N$], [MMIM]-[$(CH3)_2PO_4$] and oxygenated organic compounds respectively water. *Fluid Phase Equilib.* **2005**, *231*, 38−43.

(19) Preißinger, M.; Pöllinger, S.; Brüggemann, D. Ionic liquid based absorption chillers for usage of low grade waste heat in industry. *Int. J. Energy Res.* **2013**, *37*, 1382−1388.

(20) Calvar, N.; González, B.; Gómez, E.; Domínguez, Á Vapor−liquid equilibria for the ternary system ethanol + water + 1-butyl-3-methylimidazolium methylsulfate and the corresponding binary systems at 101.3 kPa. *J. Chem. Eng. Data* **2009**, *54*, 1004−1008.

DOI: 10.1021/acssuschemeng.5b00062
ACS Sustainable Chem. Eng. 2015, 3, 750−757

(21) SENSIRION. Datasheet SHT7x. http://www.sensirion.com/fileadmin/user_upload/customers/sensirion/Dokumente/Humidity/Sensirion_Humidity_SHT7x_Datasheet_V5.pdf (accessed 8/20/2014).
(22) Klose, B. *Meteorologie*; Springer Verlag: Berlin/Heidelberg, Germany, 2008.
(23) McNeely, L. A. Thermodynamic properties of aqueous solutions of lithium bromide. *ASHRAE Trans.* **1979**, *85*, 413−434.
(24) Dittmann, L. Beiträge zur optimalen Auslegung und Betriebsführung von Absorptions-Kältemaschinen im Systemverbund. Ph.D. Thesis, TU Dresden, Dresden, Germany, 2008.
(25) World Energy. Absorption chiller/heat pump. http://www.baxterenergy.com (accessed 8/7/2014).
(26) Yoshizawa, M.; Xu, W.; Angell, C. A. Ionic liquids by proton transfer: Vapor pressure, conductivity, and the relevance of ΔpK_a from aqueous solutions. *J. Am. Chem. Soc.* **2003**, *125*, 15411−15419.
(27) Bhatia, A. Overview of vapor absorption cooling systems. http://www.cedengineering.com/courseoutline.asp?cid=385 (accessed 5/8/2013).
(28) The Trane Company. Trane horizon absorption series two-stage steam-fired or hot water absorption water chillers. http://www.trane.com/download/equipmentpdfs/absds4.pdf (accessed 8/14/2014).
(29) Keil, P.; Kick, M.; König, A. Long-term stability, regeneration and recycling of imidazolium-based ionic liquids. *Chem. Ing. Tech.* **2012**, *84*, 859−866.

DOI: 10.1021/acssuschemeng.5b00062
ACS Sustainable Chem. Eng. 2015, 3, 750−757